DNA condensation by copper(II) complexes and their anti-proliferative effect on cancerous and normal fibroblast cells

ARTICLE *in* EUROPEAN JOURNAL OF MEDICINAL CHEMISTRY · APRIL 2014

Impact Factor: 3.45 · DOI: 10.1016/j.ejmech.2014.04.064 · Source: PubMed

3 AUTHORS:

Rajalakshmi Subramaniyam
Konan University
8 PUBLICATIONS **69** CITATIONS
SEE PROFILE

Manikantan Syamala Kiran
Central Leather Research Institute
37 PUBLICATIONS **296** CITATIONS
SEE PROFILE

Balachandran Unni Nair
Central Leather Research Institute
368 PUBLICATIONS **6,018** CITATIONS
SEE PROFILE

European Journal of Medicinal Chemistry 80 (2014) 393–406

Contents lists available at ScienceDirect

European Journal of Medicinal Chemistry

journal homepage: http://www.elsevier.com/locate/ejmech

Original article

DNA condensation by copper(II) complexes and their anti-proliferative effect on cancerous and normal fibroblast cells

Subramaniyam Rajalakshmi [a], Manikantan Syamala Kiran [b], Balachandran Unni Nair [a,*]

[a] Chemical Laboratory, Central Leather Research Institute, Council of Scientific and Industrial Research, Adyar, Chennai 600 020, India
[b] Bio-Materials Laboratory, Central Leather Research Institute, Council of Scientific and Industrial Research, Adyar, Chennai 600 020, India

ARTICLE INFO

Article history:
Received 11 January 2014
Received in revised form
17 March 2014
Accepted 22 April 2014
Available online 24 April 2014

Keywords:
Copper(II) complexes
DNA condensation
MG63 fibroblast cell
Apoptosis
Mitochondrial pathway
Oxidative stress

ABSTRACT

In our search towards copper(II) based anticancer compounds, copper(II) complexes $[Cu(bitpy)_2](ClO_4)_2$ **1**, $[Cu(bitpy)(phen)](NO_3)_2$ **2** and $[Cu(bitpy)(NO_3)](NO_3)$ **3** were synthesized and characterized. All the three complexes contain the tridentate ligand bitpy, which bears biologically relevant benzimidazolyl head group, as one of the ligands. Because of the presence of the planar benzimidazolyl group in the bitpy ligand, the complexes exhibited intercalative mode of binding with DNA. The DNA binding constant, K_b, for complexes **1**, **2** and **3** were determined to be $(1.84 \pm 0.32) \times 10^4$, $(1.83 \pm 0.57) \times 10^4$ and $(1.87 \pm 0.21) \times 10^4\ M^{-1}$ respectively. All the three complexes possessed DNA condensing ability. The DNA condensing ability of the complexes was in the order **2** > **1** > **3**. The DNA condensation induced by these three complexes was found to be reversed in the presence of 1 M NaCl. In vitro cytotoxicity of three complexes was tested against osteosarcoma MG63 cell line as well as normal fibroblast NIH3T3 cell line by MTT reduction assay. Complexes **1** and **2** were found to be highly toxic towards MG63 than NIH3T3 cell line and both these complexes brought about cell death in the MG-63 cell line due to apoptosis. Whereas, complex **3** exhibited almost equal toxic effect towards both MG63 and NIH3T3 cell lines. Based on the fact that both complexes **1** and **2** brought about reversible condensation of DNA and induced apoptosis in osteosarcoma MG-63 cell line, it is hypothesized that they might possess potential pharmaceutical applications.

1. Introduction

Coordination complexes of transition metal ions occupy an important position in medicinal biochemistry. Platinum(II) based complexes, especially cisplatin and related compounds have fascinated inorganic chemists for a long time because of their anticancerous properties [1–3]. Cisplatin and its related compounds are widely used in chemotherapy. However, one of the significant problems with cisplatin and other platinum based drugs is their chemo-resistance. To surmount this issue, numerous transition metal complexes have been synthesized and tested for their anticancer activity [4–10]. In the past, copper(II) complexes have attracted special attention because of the fact that copper is an essential trace element and is required for normal cellular activity as a cofactor for many enzymes [11–13]. Some of the earliest compounds of copper(II) to gain interest of medicinal chemists due to their anticancer property are Cu(II) complexes of thiosemicarbazones and its derivatives [14–16]. Current focus of research on copper(II) complexes stems from their multivariate use; for example copper(II)–bipyridyl and copper(II)–phenanthroline complexes have been reported to exhibit antimicrobial, antiviral, anti-inflammatory and antitumor properties [17–20]. Moreover, copper(II), nickel(II) and ruthenium(III) complexes have also been demonstrated to function as enzyme inhibitors, DNA condensing agents, DNA cross-linking agents and chemical nucleases [17,21–24]. The properties of the copper(II) complexes are largely determined by the nature of ligands and donor atoms bound to the metal ion. Currently, for biological applications, ligands for copper(II) complexes are designed in such a way that they increase the lipophilicity of the complex for easy transport through cell membrane and also facilitate their binding to DNA and proteins. A number of copper(II) and copper(III) complexes containing biologically active ligands have been reported to have anti-proliferative, anti-cancerous, anti-bacterial, nuclease mimetic and SOD mimetic properties [11,25–31]. Current bioinorganic research is focused on improving the therapeutic properties of such

* Corresponding author.
E-mail addresses: bunair@clri.res.in, bunninair@gmail.com (B.U. Nair).

http://dx.doi.org/10.1016/j.ejmech.2014.04.064
0223-5234/

complexes using bi-nuclear copper complexes as well as rationally designed mixed ligands to generate complexes with multiple functions. Recently, mixed ligand acetylacetone/quinoxaline complexes have been reported to exhibit nuclease and apoptosis-inducing activity [32–34]. Since 1999, our group has made significant efforts for the synthesis of ligands and respective metal complexes, which possess nuclease/protease activities as well as significant anti-proliferative effects [35–42]. It has been concluded from our previous studies that the cytotoxic effect of the metal complexes depends on their binding ability towards DNA. Even though a large number of copper(II) complexes have been shown to exhibit anticancer activity, only a few complexes have been reported to possess DNA condensation property. The complex $[Co(NH_3)_6]^{3+}$ has been shown to bring about DNA condensation [21]. The DNA condensing ability of this complex has been attributed to its electrostatic charge. DNA condensation ability is a prerequisite for gene therapy [43–46]. The challenge of successful gene therapy relies greatly on the development of effective and safe carrier, which is capable of compacting and delivering DNA. The DNA condensing ability is also essential for DNA transcription and replication. A molecule having both anticancer activity as well as gene targeting ability is expected to have significant application in medicinal chemistry.

In this manuscript, we describe the synthesis and characterization of three copper(II) complexes containing tridentate, bidentate and monodentate ligands. Benzimidazole (bzim) based ligand was chosen as a common ligand for all the three complexes because bzim has pharmaceutical and therapeutic applications [47]. Benzimidazole when incorporated into 4′ position of terpyridine ligand as benzimidiazolylterpyridine (bitpy), is expected to enhance the DNA binding ability due to its H-bonding ability. The efficacy of these complexes to bring about DNA condensation as well as their anti-proliferative effects on normal and cancerous fibroblast cell lines has also been examined.

2. Materials and methods

2.1. Materials

The chemicals, 2-acetyl pyridine, 1,10-phenanthroline, agarose, ethidium bromide, calf thymus DNA, 3-(4,5-dimethylthiazol-2-yl)-2,5-diphenyl tetrazolium bromide and propidium iodide were purchased from Sigma Chemical Company (St. Louis, MO, USA). Trypsin, DMSO, Tris (hydroxymethyl) methylamine and Tris-borate-EDTA were purchased from Sisco Research Laboratory (Mumbai, India). Human osteosarcoma fibroblast cell line, MG-63 and mouse embryonic fibroblast noncancerous cell line NIH-3T3 were obtained from National Centre for Cell Sciences (NCCS, Pune, India). Caspase 3 and caspase 9 were purchased from M/s R & D systems (Bangalore, India). Caspase 8 was purchased from M/s Invitrogen. Minimum Essential Medium Eagle (MEM) was purchased from Hi Media Laboratories (Bangalore, India) and fetal bovine serum (FBS) was purchased from Cistron laboratories (Hyderabad, India). Milli-Q triply deionized water was employed for all the studies. The ligand bitpy was synthesized according to the reported literature [48]. ^{1}H- and ^{13}C NMR of bitpy is given in the supplementary information (Fig. S1).

2.2. Synthesis of complex, $[Cu(bitpy)_2](ClO_4)_2\cdot 2H_2O$ (**1**)

A methanolic solution (50 mL) of $Cu(ClO_4)_2\cdot 6H_2O$ (0.18 g, 0.5 mmol) and bitpy (0.35 g, 1 mmol) was refluxed for 30 min. A green solid that separated out upon slow evaporation of the solvent was filtered, and washed with diethyl ether and dried in vacuum. The complex was recrystallized from acetonitrile-water mixture. Yield: 79%. Found: C, 52.92; H, 3.31; N, 14.13%. Anal Calcd for $C_{44}H_{34}Cl_2CuN_{10}O_{10}$: C, 52.99; H, 3.44; N, 14.05%.

2.3. Synthesis of complex, $[Cu(bitpy)(phen)](NO_3)_2\cdot 3H_2O$ (**2**)

A methanolic solution (50 mL) of $Cu(NO_3)_2\cdot 3H_2O$ (0.12 g, 0.5 mmol) and bitpy (0.15 g, 0.5 mmol) was stirred at room temperature for 30 min. Subsequently, 1,10-phen (0.12 g, 0.5 mmol) was added to the above solution and stirred continuously for another 30 min. The resulting solution was reduced under pressure to yield dark green solid. The compound was recrystallized from acetonitrile- water mixture. Yield: 72%. Found: C, 52.86; H, 3.81; N, 16.27%. Anal Calcd: for $C_{34}H_{29}CuN_9O_9$: C, 52.95; H, 3,79; N, 16.35%.

2.4. Synthesis of complex, $[Cu(bitpy)(NO_3)]NO_3\cdot H_2O$ (**3**)

The complex **3** was synthesized by following the procedure described for the synthesis of complex **1** employing bitpy (0.35 g, 1 mmol) and $Cu(NO_3)_2\cdot 3H_2O$ (0.24 g, 1 mmol). The green colored precipitate obtained was recrystallized from acetonitrile-water mixture. Yield: 72%. Found: C, 47.58; H, 3.13; N, 17.71%. Anal Calcd: for $C_{22}H_{17}CuN_7O_7$: C, 47.61; H, 3.09; N, 17.67%.

2.5. DNA binding experiments

Stock solutions of metal complexes (10 mM) were prepared by dissolving the complexes in acetonitrile (500 μL) and making up to a total volume of 5 mL using 10 mM Tris buffer (pH 7.2). Absorption spectral titration experiments were carried out for the complexes **1**, **2** and **3** by maintaining a constant concentration of the complex (20 μM) and varying the CT-DNA concentration (5–120 μM). An equal amount of DNA was added to the cell in the reference compartment.

For viscosity measurements, the Ubberhold viscometer (1 mL capacity) was thermostated in a water bath maintained at 25 °C. The flow time for each sample was measured thrice using digital stopwatch and an average flow time was calculated. The flow rate for buffer (10 mM Tris), DNA (100 μM) and DNA with the copper(II) complexes at various concentrations (5–120 μM) was measured. The relative specific viscosity was calculated using the equation, $\eta = (t - t_o)/t_o$, where t_o is the flow time for the buffer and t is the observed flow time for DNA in the absence and presence of the complex. Data are presented as $(\eta/\eta_o)^{1/3}$ versus $1/R$ {$R = [complex]/[DNA]$}, where η is the viscosity of DNA in the presence of the complex and η_o is the viscosity of DNA alone [49,50].

Circular dichroic spectra were recorded with a Jasco J-815 spectropolarimeter at 25 °C using 0.1 cm path quartz cell. The concentration of CT-DNA (100 mM) was kept constant and the concentration of complexes **1**, **2** and **3** varied from 5 to 120 μM. The spectra were recorded in the spectral region of 220–300 nm.

Electronic spectra were recorded using a Perkin–Elmer Lambda 35 double beam spectrophotometer. Electrospray ionization mass spectra (ESI-MS) were obtained from Thermo Finnigan LCQ 6000 advantage max ion trap mass spectrometer using acetonitrile as carrier solvent. A stock solution of DNA was prepared by stirring DNA sample dissolved in 10 mM Tris HCl buffer (pH 7.2) at 4 °C and used within 4 days of preparation. The solution was exhaustively dialyzed against Tris buffer for 48 h and filtered using a membrane filter obtained from Sartorius (0.45 μM). The filtered DNA solution in the buffer gave a UV absorbance ratio (A_{260}/A_{280}) of about 1.9, indicating that the DNA was sufficiently free from proteins [51]. The concentration of DNA was determined using an extinction coefficient of 6600 M^{-1} cm^{-1} at 260 nm [52]. All further experiments were carried out employing the prepared DNA solution in Tris buffer at pH 7.2.

2.6. DNA condensation experiments

Particle size measurements were performed by Dynamic Light Scattering (DLS) analysis using a Malvern Instrument. In the present case, DLS technique was used to investigate DNA condensation in solutions in the presence of different concentrations of complexes **1**, **2**, and **3**, respectively. The measurements were performed with 10 μM DNA in Tris buffer (50 mM, pH 7.4) at 25 °C in the presence of 2, 4, 6, 8 and 10 μM concentration of respective complexes.

Condensation of DNA by copper(II) complexes was also monitored by agarose gel electrophoresis technique. DNA condensation of all the three complexes was examined by mixing varying concentration of complexes with DNA and loading onto the wells. Plasmid DNA (pUC 18) was incubated with different concentrations (20, 40, 60, 80, 100, 120, 140 and 160 μM, respectively) of the three copper(II) complexes for 1 h at 37 °C. In a separate experiment, plasmid DNA was incubated with 40 μM of complex **1**, complex **2**, complex **3** and 50 μM solution of sodium azide for 1 h. A loading buffer containing 0.25% bromophenol blue, 40% (w/v) sucrose and 0.5 M EDTA was added to the samples and electrophoresis of DNA was performed on 0.8% agarose gel containing 0.5 μg/mL ethidium bromide. The gels were run at 50 V for 2 h in Tris–boric acid–ethylenediamine tetra acetic acid (TBE) buffer at pH 7.4. The bands were visualized by placing the gel on UV illuminator and photographed using gel documentation system.

2.7. In vitro assay for cytotoxicity

The cytotoxic effects of complexes **1**, **2**, **3**, bitpy ligand and cisplatin on MG-63 and NIH-3T3 cells were determined by MTT assay. Cells (1×10^5/well) were plated in 100 μL of medium/well in 96-well plates. Usually, after 48 h of incubation cells reach the state of confluence. In the present experiment, after the confluence state, the cells were incubated with DMSO solution (5, 10, 20, 40, 60 and 100 μM, respectively) of the three complexes, ligand bitpy (5, 10, 20, 40, 60 and 100 μM, respectively) and cisplatin (5, 10, 20, 40, 60 and 100 μM, respectively) in Tris buffer for 48 h at 37 °C. After removal of the sample solution and washing with phosphate-buffered saline (pH 7.4), 20 μL/well (5 mg/mL) of 0.5% 3-(4,5-dimethyl-2-thiazolyl)-2,5-diphenyl-tetrazolium bromide (MTT) phosphate-buffered saline solution was added. After 4 h incubation, 10% DMSO was added into the wells. Cell viability was determined by measuring the absorbance at 570 nm. The concentration of the copper(II) complexes required to achieve 50% inhibition of viability (IC_{50}) was determined graphically. The absorbance at 570 nm was also measured for wells without any sample as blank. The effect of copper(II) complexes on proliferation of MG-63 and NIH-3T3 was expressed as % cell viability, using the following formula

$$\%\ \text{cell viability} = A_{570\ \text{nm}}\ \text{of treated cells}/A_{570\ \text{nm}}\ \text{of control cells} \times 100\%$$

To detect apoptosis, annexin-V antibody conjugated with fluorescent dye, fluorescein isothiocyanate was employed for the experiment. The kit uses a staining protocol in which the early apoptotic cells are stained with annexin-V (green fluorescence), which has excitation wavelength (λ_{ex}) of 488 nm and emission wavelength λ_{em} of 520 nm. Late apoptotic cells were stained with propidium iodide (red fluorescence) which has λ_{ex} of 540 nm and λ_{em} of 630 nm. Viable cells were neither Annexin V nor propidium iodide positive. The cells were grown to 70% confluence and treated with complexes **1** and **2** for 24 h. Cells that had bound FITC-annexin V and excluded propidium iodide were termed as early apoptotic cells; whereas cells which could permeate propidium iodide (regardless of presence of absence of bound FITC-annexin V) were deemed as late apoptotic.

2.8. Caspase 3 and 9 enzyme activity assay

Activity of caspase 3 and 9 was measured using the colorimetric caspase 3 and 9 assay kits from M/s Invitrogen. After exposure to varying concentration of complexes **1**, **2** and **3**, cells were sampled for cleavage of caspase 3 and 9 as per the manufacturer's instructions. Briefly, adherent cells were washed with cold PBS, collected with a cell scraper, and suspended in cell lyses buffer. After incubation for 10 min on ice and subsequent centrifugation, protein concentrations of the supernatants were measured according to Bradford's method. Samples (equivalent amount in μg protein extract, respectively) were subjected to caspase 3 and 9 activities as directed in manufacturer's manual.

2.9. Caspase 8 colorimetric assay

Caspase 8 activity was measured using M/s Invitrogen Caspase colorimetric assay Kit. Briefly, 5×10^6 cells (NIH3T3 and MG63 cells) were seeded in a 25 mm^2 culture flask. Cells were allowed to grow overnight. Medium was removed and fresh medium containing complex **1** and **2** at a concentration of 10 μM was supplemented to the cells. After 6 h, the medium was removed and cells were isolated by trypsinization. The caspase activity was measured following the manufacturer's instruction and caspase 8 activity was expressed as OD units per mg protein.

2.10. DCFH-DA fluorescence microscopic assay for measuring redox state of cell

Cells at a concentration of 7000 cells/well were seeded in a 12 well culture plate. The cells were allowed to grow until 50% confluency was achieved. Subsequently, the cells were then treated with 5 and 10 μM concentration of complexes **1** and **2**, respectively and maintained in culture for 10 h. Cells were then washed and incubated with 5 μM-dichlorofluorescin diacetate H_2 in either PBS or DMEM for 30 min in dark [53]. After incubation, the cells were resuspended in fresh PBS after thorough washing with PBS. Images of the cells were taken using (495 nm excitation and 523 nm emission) Leica fluorescent microscope employing blue filter.

2.11. Hemolysis assay

Blood sample (5 mL) was collected from healthy volunteer in a tube containing heparin. Sample was centrifuged at 1500 rpm for 5 min to remove the buffy coat as well as the plasma. The RBC was washed twice with 150 mM NaCl and finally the RBC was suspended in PBS buffer solution. Various concentrations of complexes to be tested were pipetted out into centrifuge tubes and final volume of each solution was made up to 800 μL using PBS. To all the tubes, 200 μL of RBC solution was added and gently mixed and the same solution was incubated at 37 °C for 1 h. DMSO alone as a control was also tested. In addition, positive and negative controls were also employed, where RBC in double distilled water served as a positive control and RBC in PBS served as a negative control.

3. Results and discussion

3.1. Synthesis and characterization of the complexes

Complex **1** was synthesized from bitpy ligand and $Cu(ClO_4)_2 \cdot 6H_2O$. Complex **2** was synthesized from bitpy and phen with $Cu(NO_3)_2 \cdot 3H_2O$ as a source for copper(II). Complex **3** was

synthesized from the reaction of bitpy and $Cu(NO_3)_2 \cdot 3H_2O$ in methanol solution. ESI mass spectrum of complex **1** exhibits base peak at *m/z* 380.53 indicating the presence of complex cation $[Cu(bitpy)_2]^{2+}$. The ESI mass spectrum of complex **1** also exhibits peak at *m/z* 412.20 and 512.93, which can be assigned to $[Cu(bitpy-H)]^{+}$ and $[Cu(bitpy)](ClO_4)^{+}$, respectively. Molecular ion peak observed in the mass spectrum of complex **2** at *m/z* 296.27 is indicative of complex cation, $[Cu(bitpy)(phen)]^{2+}$. This complex also exhibit peaks at *m/z* 474.13 and 654.47, which can be assigned to $[Cu(bitpy)(NO_3)]^{+}$ and $[Cu(bitpy)(phen)(NO_3)]^{+}$, respectively. The base peak observed in the mass spectrum of complex **3** at *m/z* 474.07 is indicative of complex cation, $[Cu(bitpy)(NO_3)]^{+}$. The mass spectrum of this complex also shows peak at *m/z* 226.47, which can be attributed to $[Cu(bitpy)(CH_3CN)]^{2+}$. The ESI-MS of complexes **1**, **2** and **3** are given in the supplementary information (Fig. S2). The schematic representation of the synthesis of complexes **1**, **2** and **3** are shown in Scheme 1. The tridentate bitpy forms a bis complex with Cu(II) in the case of complex **1** as has previously been reported for $[Cu(itpy)_2]$ $(ClO_4)_2$ complex by our group [54]. The tridentate bitpy and bidentate phen with copper(II) forms $Cu(II)N_5$ type complex **2**. Similar $Cu(II)N_5$ type of complex, $[Cu(ptpy)(dmp)]^{2+}$ has previously been reported [55]. Complex **3** with bitpy forms a four coordinate complex with copper(II), as has been reported in the case of [Cu(itpy)Cl]Cl [56].

The UV–Visible spectrum of acetonitrile solution of complex **1** shows strong CT band at 354 nm ($\varepsilon = 4.7 \times 10^4$ M^{-1} cm^{-1}) and intraligand transition at 287 ($\varepsilon = 3.4 \times 10^4$ M^{-1} cm^{-1}) and 270 nm ($\varepsilon = 2.7 \times 10^4$ M^{-1} cm^{-1}). The corresponding transitions for complex **2** have been observed at 355 ($\varepsilon = 2.25 \times 10^4$ M^{-1} cm^{-1}) and 270 nm ($\varepsilon = 4.0 \times 10^4$ M^{-1} cm^{-1}) and for complex **3**, at 355 ($\varepsilon = 2.7 \times 10^4$ M^{-1} cm^{-1}) and 288 nm ($\varepsilon = 2.1 \times 10^4$ M^{-1} cm^{-1}), respectively. All the three complexes also exhibit low intensity ligand field transition around 550–800 nm. Generally, six coordinate as well as five coordinate copper(II) complexes are expected to exhibit $d_{xz,yz} \rightarrow d^{22}_{x-y}$ and $d^{2}_{z} \rightarrow d^{22}_{x-y}$ transitions. However, in most cases only two bands or a single broad band is observed due to the fact that energy of the three transitions is close to one another. In the case of square planar complexes, the energy of $d_{xz,yz} \rightarrow d^{22}_{x-y}$ transitions are very close and as a result one expects only two transitions. Moreover, in the present case if the energy of the two transitions is close to one another, one can observe only one broad transition. Complex **1** exhibits a weak and relatively sharp ligand field band centered at 583 nm ($\varepsilon = 120$ M^{-1} cm^{-1}), which can be attributed to $d_{xz,yz} \rightarrow d^{22}_{x-y}$ transition and a broad band with λ_{max} around 678 nm ($\varepsilon = 80$ M^{-1} cm^{-1}) which results from two transitions namely, $d_{xy} \rightarrow d^{22}_{x-y}$ and $d^{2}_{z} \rightarrow d^{22}_{x-y}$. Complex **2** also exhibits qualitatively similar ligand field transitions as observed for complex **1**. It shows a relatively sharp spectral band centered at 580 nm ($\varepsilon = 240$ M^{-1} cm^{-1}) and a broad band with λ_{max} around 656 nm ($\varepsilon = 190$ M^{-1} cm^{-1}). The ligand field transitions of complexes **1** and **2** clearly suggest six coordinate and five coordinate geometries for these two complexes, respectively. On the contrary the ligand field transition of complex **3** was different from that observed for other two complexes. This complex showed only one broad band centered at 678 nm ($\varepsilon = 180$ M^{-1} cm^{-1}), which can be assigned to $d_{xz,yz} \rightarrow d^{22}_{x-y}$ and $d^{2}_{z} \rightarrow d^{22}_{x-y}$ transitions and a shoulder at around 728 nm, which can be assigned to $d_{xy} \rightarrow d^{22}_{x-y}$ transition.

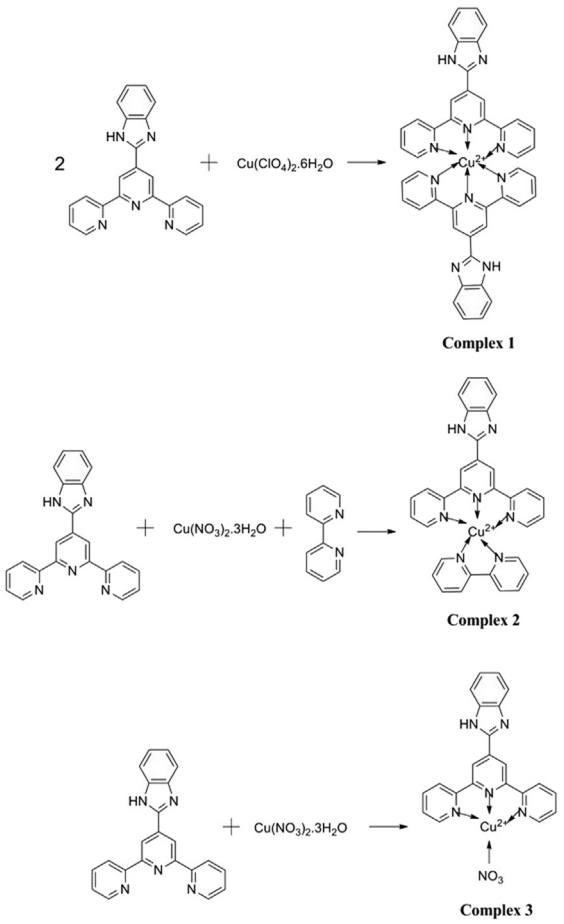

Scheme 1.

3.2. DNA binding studies

3.2.1. Electronic spectral studies

Absorption titration method has been employed to monitor the interaction of the three complexes with Calf Thymus (CT)-DNA. The absorption spectrum of 20 μM of complex **1**, **2** and **3** in the absence and presence of CT-DNA are shown in Fig. 1. It is clearly seen from the spectra that binding of respective copper(II) complexes to DNA lead to perturbation in their ligand centered band. A strong hypochromic effect in the intraligand transition was observed for all the three complexes upon addition of incremental amount of DNA (0–100 μM). Clear isosbestic points at 376 nm for complexes **1**–**3** was observed in the spectral changes during the absorption titration. This observation clearly illustrates the existence of only two species, free complex and DNA bound complex in solution. The spectral changes observed in all the three cases are clearly indicative of intercalative binding of the three complexes to DNA [57]. Since the complexes possess aromatic ring (bitpy) which can π-stack between the DNA base pairs, the intercalative binding of the three complexes to DNA is not surprising. In order to compare quantitatively the binding affinity of complexes **1**, **2** and **3** to CT-DNA, the intrinsic binding constant K_b of the complexes was determined by monitoring the changes in absorbance of the intraligand bands with increasing concentration of CT-DNA [58]. The K_b has been calculated from equation;

$$[DNA]/(\varepsilon_a - \varepsilon_f) = [DNA]/(\varepsilon_b - \varepsilon_f) + 1/K_b(\varepsilon_b - \varepsilon_f) \quad (1)$$

where ε_a, ε_f, and ε_b correspond to A_{obsd}/[Cu(II) complex], the extinction coefficient for free copper(II) complex and the extinction coefficient for the copper(II) complex in the fully bound form, respectively [59]. A plot of $[DNA]/(\varepsilon_a - \varepsilon_f)$ versus [DNA], gives K_b as the ratio of the slope to the intercept. The binding constant K_b of complexes **1**, **2** and **3** was determined to be $(1.84 \pm 0.32) \times 10^4$, $(1.83 \pm 0.57) \times 10^4$ and $(1.87 \pm 0.21) \times 10^4$ M^{-1}, respectively. These values are similar to

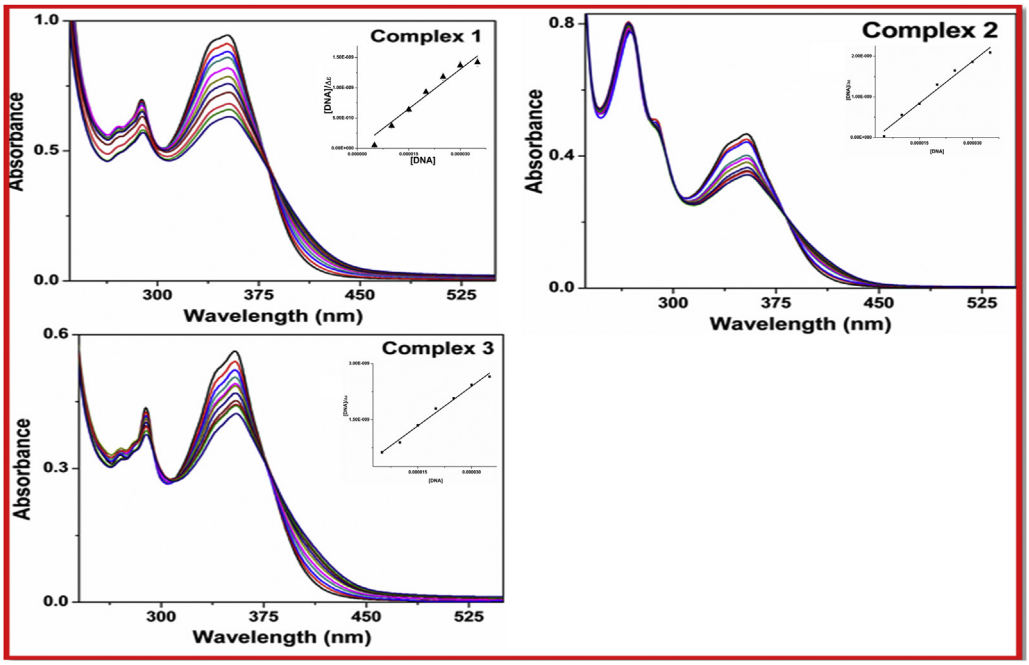

Fig. 1. Absorption spectral titration of complex **1**, **2** and **3** (10 μM) in Tris buffer solution with increasing concentration of CT-DNA (5–120 μM).

those reported for [Ni(hydrazine)(triphenylphosphine)]$^{2+}$, [Ni(10,12-Dimethyl_pteridino[6,7-f][1,10]phenanthroline-11,13(10H, 12H)-dione)$_2$]$^{2+}$ and [Ru(bipyridine)$_2$(11,13-dimethyl-13H-4,5,9,11,14-hexaaza-benzo[b]triphenylene-10,12-dione]$^{2+}$ which have been shown to bind intercalatively to DNA [38,60,61]. It is intriguing to note very minor difference in the K_b values of the three complexes, and the reason being the presence of the bitpy ligand, which dictates the mode of binding of these complexes to DNA.

3.2.2. Viscosity studies

To further investigate the nature of binding of complexes to DNA, viscosity measurements of the solutions of DNA incubated with the complexes were carried out. In the viscosity measurements, the rate of flow of the buffer (10 mM Tris), DNA (100 μM) and DNA with the copper(II) complexes at various concentrations (0–100 μM) were measured. The relative specific viscosity was calculated using the equation $(t - t_o)/t_o$, where t_o is the flow time for the buffer and t is the observed flow time for DNA in the absence and presence of the complex. Data are presented as $(\eta/\eta_o)^{1/3}$ vs $1/R$ {R = [complex]/[DNA]}, where η is the viscosity of DNA in the presence of complex and η_o is the viscosity of DNA alone (Fig. 2). In all the three cases, the viscosity of DNA was found to increase with increase in the concentration of the metal complex. In the presence of complex **1**, a gradual increase in DNA viscosity with increase in the concentration of the complex was observed and saturation was attained at a concentration of 70 μM. In the case of complex **2**, an increase in the viscosity of DNA was observed even at the concentration of 100 μM. In the presence of complex **3**, a four coordinate complex, viscosity of DNA exhibited an appreciable increase with increase in the concentration of the complex. Classical intercalators like ethidium bromide (EB) cause lengthening of the DNA duplex upon the insertion of EB between the stacked bases, and this further increases the relative viscosity of DNA. On the other hand, if the DNA binding molecule bends or kinks the DNA helix, which is attributed to the strong covalent binding of complexes with DNA bases, decrease in the specific viscosity of DNA can be expected [62]. The viscosity data clearly demonstrates intercalative mode of binding of complexes **1**, **2** and **3** to DNA.

3.2.3. Circular dichroic spectral studies

Circular dichroic studies are useful in diagnosing changes in the conformation of DNA during metal complex-DNA interactions [63]. The characteristic CD spectrum of CT-DNA (100 μM) consists of a positive band at 280 nm due to base stacking and a negative band at 244 nm due to helicity and is characteristic of DNA in right-handed B-form [64]. Intercalators are known to alter the intensities of both these bands, with consequent stabilization of right-handed B conformation of DNA. An increase in positive and a decrease in negative ellipticity indicate strong conformational changes in DNA [65]. Incubation of complexes **1**–**3** (0–100 μM) with DNA led to notable changes in the positive and negative bands in the CD spectrum of DNA (Fig. 3). CD spectrum of DNA in the presence of

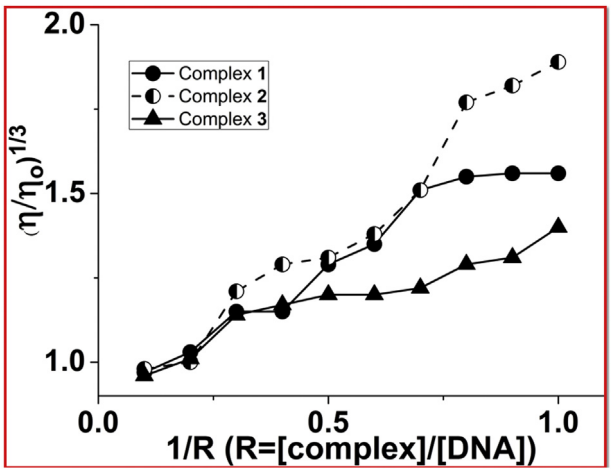

Fig. 2. Effect of complexes **1, 2** and **3** (5–120 μM) on the relative specific viscosity of CT-DNA (100 μM) in Tris buffer.

complex **1** shows a decrease in the intensity of the positive band, with 3–4 nm red shift in the position of the band and an increase in the intensity of the negative band, with a 7 nm red shift. In the presence of complex **2**, the CD spectrum of DNA shows an increase in intensity of both negative and positive bands with a shift of 7 nm towards lower energy in the positive band and a small shift of 2 nm in the negative band. Furthermore, in the presence of complex **3**, an increase in the intensities of both the bands of DNA was observed (Fig. 3). The CD spectrum clearly demonstrates red shift in both the bands; 2–3 nm shift in the positive band and 5 nm shift in the negative band. These observations clearly indicate intercalative binding of these complexes to DNA. It is also indicative that binding of complexes **1** and **3** led to larger changes in the helicity of DNA when compared to changes induced by complex **2**.

3.3. Gel electrophoresis assay

Agarose gel electrophoresis actually gives information on size-charge ratio. The ability of each of the three complexes to condense plasmid DNA was evaluated by gel electrophoresis assay. Retardation of DNA bands in the gel can indicate the decrease in the negative charge on the plasmid DNA and the formation of large-sized DNA particles [23,66]. Retardation of supercoiled DNA on the loading wells in the presence of copper(II) complexes is shown in Fig. 4. It can be seen from Fig. 4a that complexes **1** and **2** brought about condensation of DNA. However, in the presence of 10 μM complex **1**, no DNA condensation was observed; it only promoted nicking of DNA. In the case of 10–40 μM complex **2**, apart from inducing DNA condensation the complex also promoted some nicking of DNA (Fig. 4b). Nevertheless, at higher concentration, complex **2** brought about only DNA condensation. This observation could be explained based on the fact that increase in the metal complex concentration leads to neutralization of the negative charge of phosphate function of DNA as well as an increase in the size of DNA due to adduct formation with the metal complex. Furthermore, complex **3** also brought about DNA condensation but only at higher concentrations (>50 μM). This complex unlike the other two complexes was more effective in bringing about DNA cleavage as can be seen in respective gel electrophoretogram (Fig. 4c). Complex **3** is a four coordinate complex and as a result one can expect it to interact coordinatively with phosphate group of DNA, thereby promoting hydrolytic cleavage of DNA as observed in the present case (Fig. 4c). It can be seen from Fig. 4c, that with increase in concentration, complex **3** brought about cleavage of plasmid DNA from Form I (supercoiled form) to Form II (nicked circular). To test the reversibility of DNA condensation brought about by complexes **1**–**3**, 1 M NaCl was added to DNA treated with the three complexes (data not shown). The solution to which 1 M NaCl was added was also subjected to electrophoresis. DNA treated with all the three complexes showed mobility on the gel. It is highly apparent from the observed data that DNA condensation brought about by the three complexes was reversible. The release of DNA from its compact state is very important for efficient non-viral gene vectors [43,67]. The ability to reversibly condense DNA is a pre-requisite for being an effective vector [68].

3.4. Dynamic light scattering

Dynamic light scattering (DLS) is a powerful tool for measuring particle size distributions in solution [69]. In the present study, DLS technique was used to investigate DNA condensation in solution in the presence of different concentrations of complexes **1**, **2** and **3**. The measurement was performed at 10 μM DNA concentration in Tris buffer at 25 °C. Under this condition, the hydrodynamic diameter of DNA was found to be 1035 ± 50 nm. The hydrodynamic diameter of DNA condensed by complexes **1**, **2** and **3** is shown in Fig. 5. It can be seen from the figure that all the three complexes were able to induce DNA condensate formation. In the case of complex **1**, at [complex]/[DNA] ratio of 0.2, the observed hydrodynamic radius of DNA was 598 nm. This value gradually increased

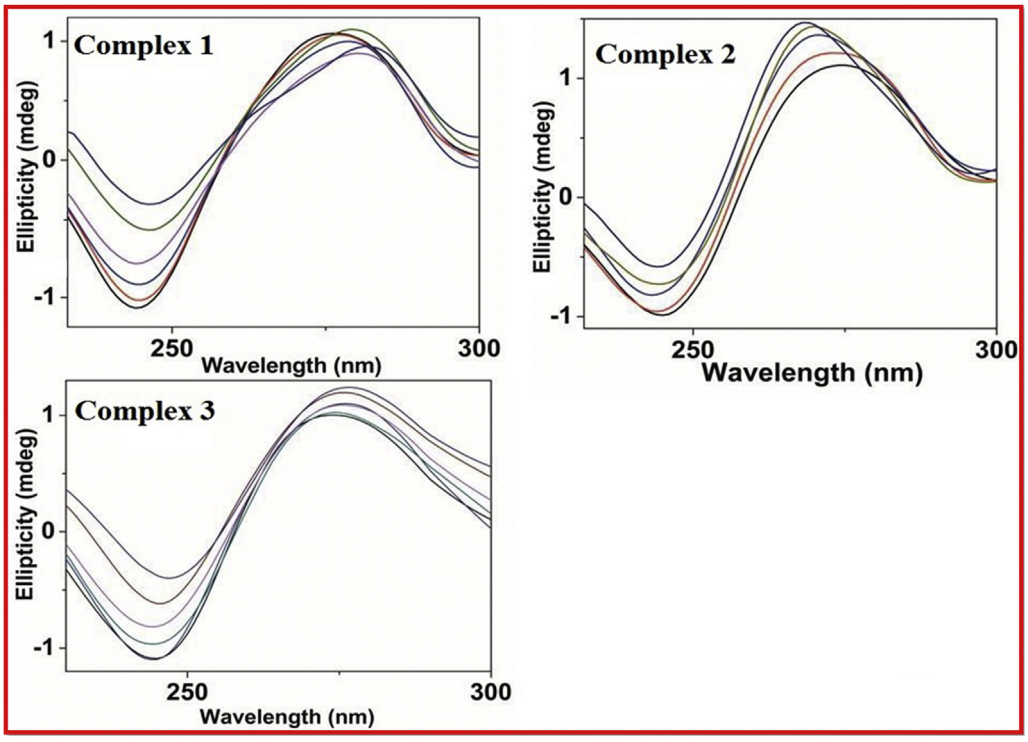

Fig. 3. Circular dichroism spectra recorded over the wavelength range of 220–300 nm of CT-DNA (20 μM) in the presence of complex **1**, complex **2** and complex **3** (5–100 μM).

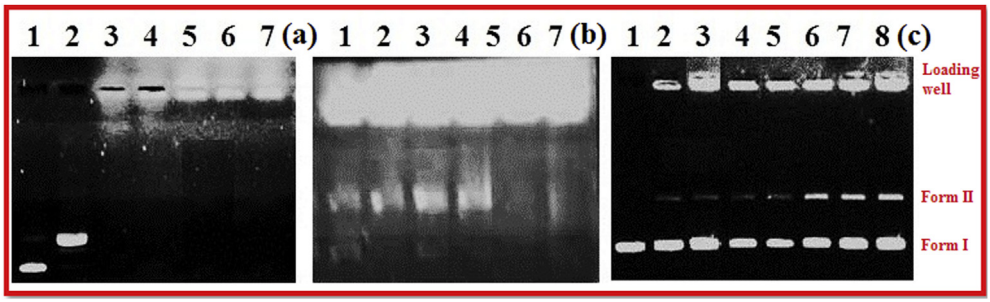

Fig. 4. (a) Gel retardation assay of complex **1** incubated with pUC 18 DNA (200 ng) for 60 min in Tris buffer (pH 7.2). Lane 1, DNA control; lane 2, DNA + 1 (10 μM); lane 3, DNA + 1 (20 μM); lane 4, DNA + 1 (30 μM); lane 5, DNA + 1 (40 μM); lane 6, DNA + 1 (50 μM); lane 7, DNA + 1 (60 μM). (b) Gel retardation assay of complex **2** incubated with pUC 18 DNA (200 ng) for 60 min in Tris buffer (pH 7.2). Lane 1, DNA + 2 (10 μM); lane 2, DNA + 2 (20 μM); lane 3, DNA + 2 (30 μM); lane 4, DNA + 2 (40 μM); lane 5, DNA + 2 (50 μM); lane 6, DNA + 2 (60 μM); lane 7, DNA + 2 (70 μM). (c) Gel retardation assay of complex **3** incubated with pUC 18 (200 ng) for 60 min in Tris buffer (pH 7.2). Lane 1, DNA control; lane 2, DNA + 3 (10 μM); lane 3, DNA + 3 (20 μM); lane 4, DNA + 3 (30 μM); lane 5, DNA + 3 (40 μM); lane 6, DNA + 3 (50 μM); lane 7, DNA + 3 (60 μM); lane 8, DNA + 3 (70 μM).

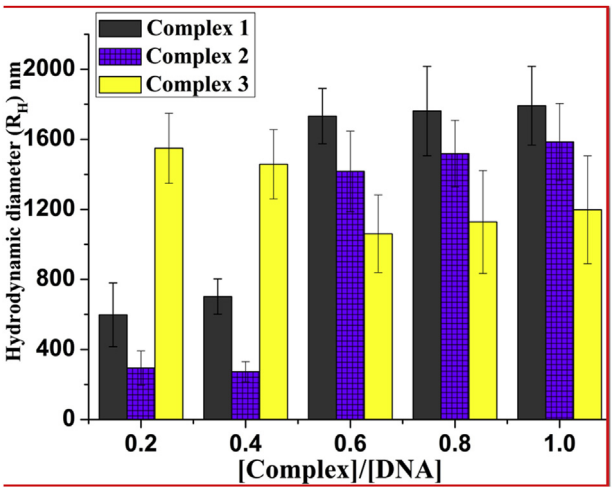

Fig. 5. Hydrodynamic diameter of DNA condensate versus the ratio of DNA to complexes **1**, **2** and **3** concentration by Dynamic Light Scattering.

to1762 nm at the [complex]/[DNA] ratio of 0.8. In presence of complex **2**, the hydrodynamic radius of the DNA condensate was found to increase from 294 nm to 1585 nm as the [complex]/[DNA] ratio was raised from 0.2 to 0.8. Whereas in the case of complex **3**, even at [complex]/[DNA] ratio of 0.2 the formation of particles with hydrodynamic radius of 1500 nm was observed. This size decreased to around 1100 nm at [complex]/[DNA] ratio of 1.0. The observed decrease in size of DNA condensate at higher [complex]/[DNA] ratio was probably due to the fact that higher concentration of complex **3** led to DNA cleavage. These results clearly demonstrate the DNA condensing ability of the three complexes.

3.5. Cytotoxicity studies

3.5.1. MTT assay

As potential gene vectors, DNA condensing agents are desired to have low toxic effect on cell lines. The cytotoxicity of complexes **1**, **2** and **3** on osteosarcoma MG63 fibroblast cell line and normal fibroblast cell line NIH3T3 was measured by MTT reduction assay [70]. MTT assay has been widely used to measure the cell proliferation rate based on the fact that live cells reduce yellow MTT to

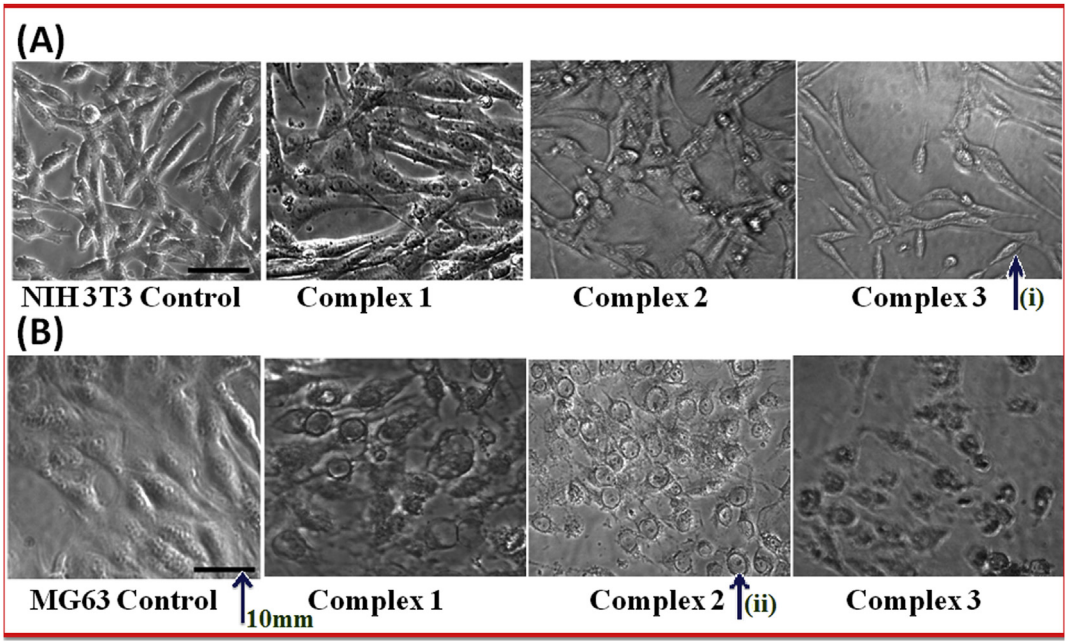

Fig. 6. Morphological changes observed in the MG-63 and NIH-3T3 cell lines on treatment with complexes **1, 2** and **3**.

blue formazan products. Further, this assay indirectly suggests the metabolic status of the cells and the events that lead to necrosis or apoptosis. In the present cytotoxic analysis, various doses such as 5, 10, 20, 40, 60, and 100 μM of copper(II) complexes were tested for their effect on cell viability and proliferation using MTT assay and the results are presented (Supplementary Information, Fig. S3) for the complexes **1**–**3**, respectively. Variance in cell growth inhibition among three complexes and a concentration dependent cell growth inhibitory effect was evident from the assay. It is anticipated that the efficacy of these complexes for therapeutic application will depend on the nature of interaction of complexes with normal and cancerous fibroblast cell lines. A potential compound with therapeutic efficacy should be able to specifically kill cancerous cells while sparing normal cells. We observed that the therapeutic efficacy of these complexes were in the order complex **1** > complex **2** > complex **3**. In the case of complex **1**, concentrations up to 20 μM had no cytotoxic effect on normal fibroblast cell line (NIH3T3), whereas only 20% viability was observed in the case of osteosarcoma MG63 cell line at a concentration of 5 μM. The IC_{50} value for complex **1** for NIH3T3 was 60 μM. For complex **2**, the IC_{50} for NIH3T3 cell line was 5 μM and only 15% viability for MG63 cell line was observed at same concentration. Complex **3** exerted cytotoxic effect on both NIH3T3 and MG63 cell line by following a similar pattern. Significant cytotoxic effect was evident even at lower concentration of 5 μM for both NIH3T3 and MG63 cell lines indicating its inapplicability in therapeutic applications. In order to further understand the IC_{50} values for complex **1** and **2** on MG63 cell line we performed MTT assay at nanomolar concentration for complexes **1** and **2**; complex **3** was omitted from further studies since the pattern of growth inhibition was similar in both NIH3T3 and MG63 cell lines. The IC_{50} values for complexes **1** and **2** for MG63 cell line was found to be 1.0 μM (1000 nM) and 1.2 μM (1200 nM), respectively (Supplementary Information, Fig. S4). Cell viability was also analyzed by including control cisplatin and the free ligand (bitpy) (Supplementary Information, Fig. S5). Although complexes **1**–**3** exerted inhibitory effect on the proliferation and growth of MG63 and NIH3T3 cells, we did not observed any inhibitory effect on MG63 cell proliferation and only marginal inhibitory effect on NIH3T3 cell proliferation was observed at a ligand concentration of 100 μM. On the other hand, 5 μM cisplatin

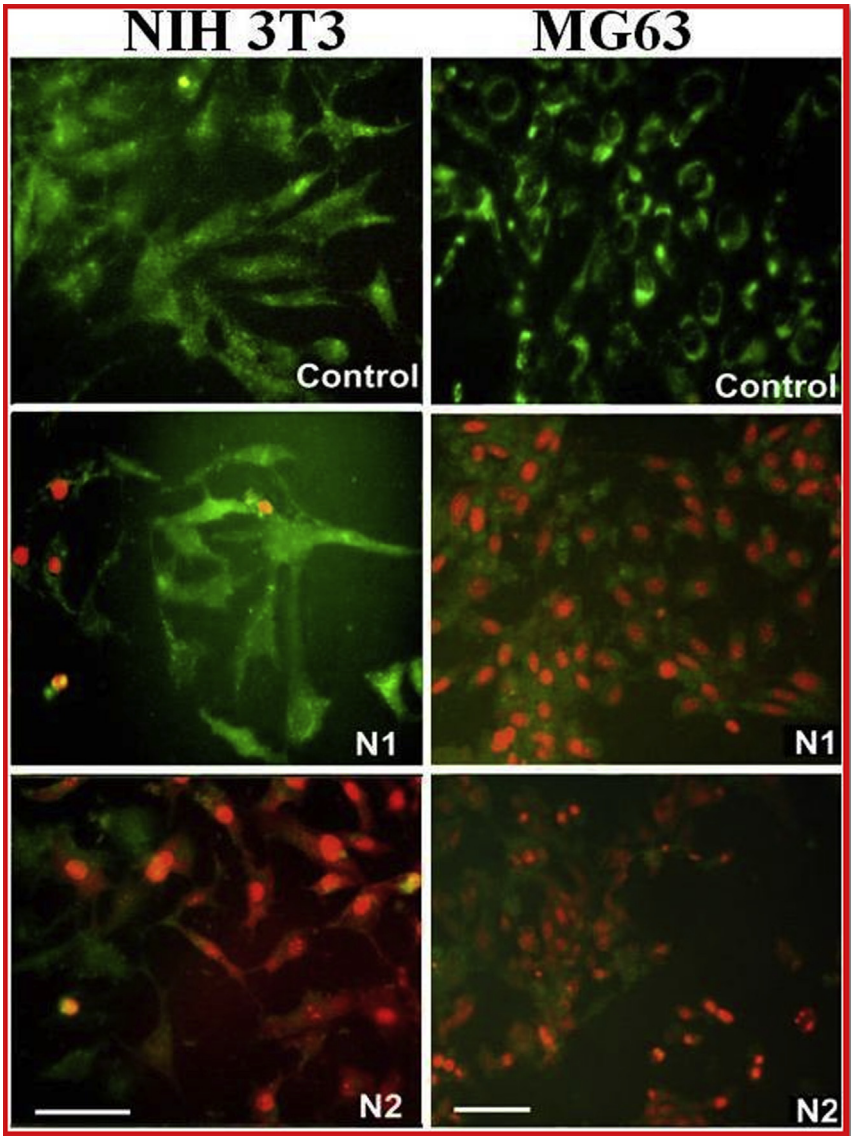

Fig. 7. Annexin V-PI stained MG-63 and NIH-3T3 cell lines treated with complex **1** (represented as **N1**) and complex **2** (represented as **N2**).

demonstrated around 80% viability in MG63 cells. The IC_{50} value for cisplatin for MG63 was observed to be at 30 μM. The obtained data clearly indicates complexes **1** and **2** as more potent inhibitors of MG63 cell proliferation when compared to cisplatin. The micro-photographs of cells treated with 5 μM solution of complexes **1**, **2** and **3** are shown in Fig. 6 (The micrographs of cells treated with different concentrations of the three complexes are provided in Supplementary Information, Fig. S6). Morphological changes, nuclear shrinkage and condensation were observed in cells at concentrations of complexes that exhibited growth inhibition. The morphological changes and nuclear condensation observed in MG63 and NIH3T3 cells were consistent with the pattern of growth inhibition observed in MTT assay. Any compound to be developed as a successful anti-cancer agent should have the ability to distinguish normal from malignant cells and selectively inhibit the growth of the malignant cell. Based on the MTT assay results, complexes **1** and **2** are proposed as potential candidates for anti-cancer therapy. The growth inhibitory effect of these complexes at low concentration was significantly high for MG63 cell line when compared to the normal fibroblast NIH3T3 cell line; at low concentrations of these two complexes the viability and proliferation of the normal fibroblast cell line NIH3T3 was not affected. The cell growth inhibition observed in MTT assay may be due to cell death either due to apoptosis (programmed cell death) or necrosis. Another possibility of cell growth inhibition may be due to cell cycle arrest caused by these complexes. However, it is unlikely that cell growth inhibition is due to cell cycle arrest, since the micro-photograph of the cells treated with various concentrations of complexes **1**–**3** clearly indicates morphological changes, which resemble cell death [71]. In order to further understand the mechanism underlying cell growth inhibition, we analyzed the apoptotic effects of complexes **1** and **2** using annexin-propidium iodide staining.

3.5.2. *Annexin V–propidium iodide staining*

Annexin V-FITC and propidium iodide (PI) staining was performed to analyze morphological assessment of cell death [72]. Viable cells do not get stained with PI since the membranes of intact cells are impermeable to PI, whereas the membranes of dead and damaged cells are permeable to PI. Cells that are in late apoptotic stage or already dead are FITC-Annexin V and PI positive. The results of the Annexin-PI staining on cells treated with complexes **1** and **2** are presented in Fig. 7. The MG63 and NIH3T3 cells treated with complexes **1** and **2** (5 μM) and stained with annexin–PI showed morphological changes, which are characteristics of apoptosis. The characteristic phenomena of apoptosis like cell shrinkage, nuclear condensation and nuclear fragmentation were observed suggesting late apoptotic cell death in MG63 cells. The effect of these complexes on NIH3T3 cells was less when compared with MG63 cells. The results observed were consistent with the

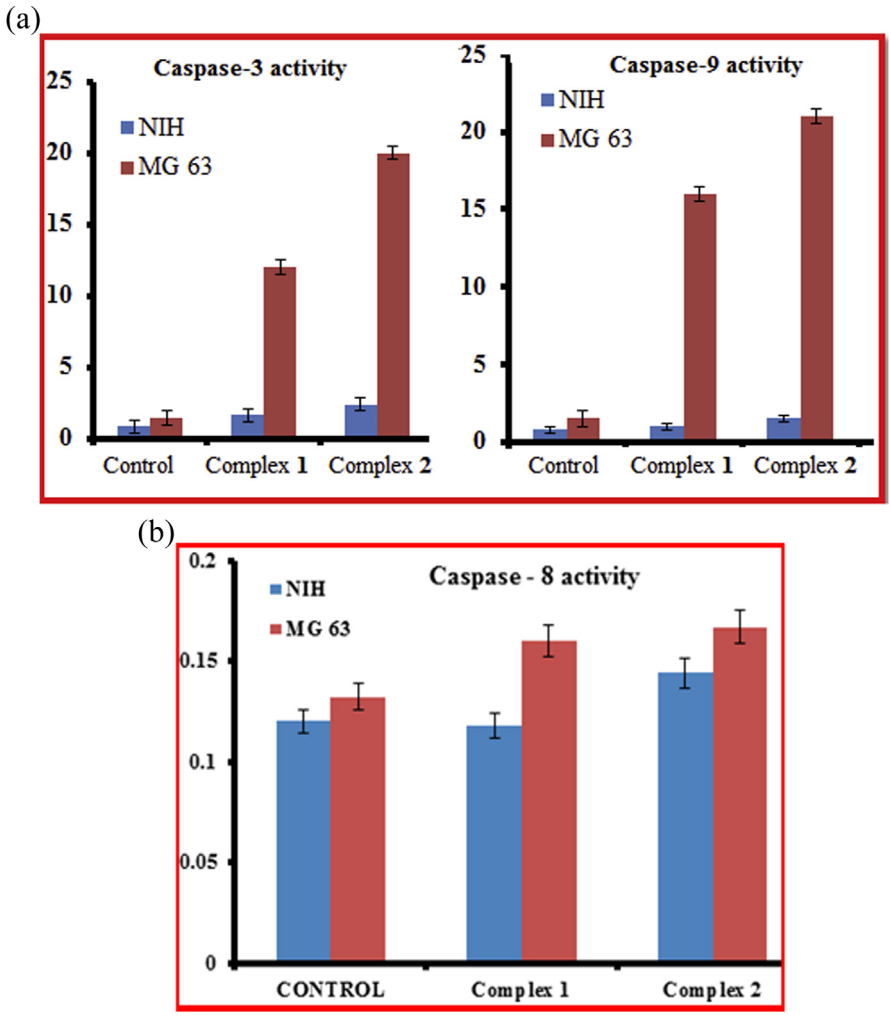

Fig. 8. (a) Effect of complex **1** and **2** on Caspase-3 activity (b) Effect of complex **1** and **2** on Caspase-9 activity.

MTT data. Complexes **1** and **2**, which are six coordinate and five coordinate respectively, showed greater cytotoxic effects on cancerous cell lines, whereas complex **3**, which is a four coordinate complex, showed almost similar effects on both normal and MG-63 cell line. Compared to the six coordinate complex **1**, the five coordinate complex **2**, which is a mixed ligand complex, showed greater effect on MG-63. A similar trend was observed in the DNA condensing property of complexes **1** and **2**.

3.5.3. *Effect of complexes 1 and 2 on caspase 3, 9 and 8*

In order to further understand the signaling events leading to apoptosis, the activity of caspase 3, 9 and 8 was analyzed. Caspases are cysteine-dependent aspartate-specific proteases that play key role in apoptotic pathways. Two types of caspases: initiator caspases, caspase 8, 10, 9, 2 and effector caspases, caspase 3, 7, 6 are reported to play key role in mediating apoptosis [73,74]. The activation of initiator caspases is required to activate specific effector caspases that subsequently proteolytically degrade a host of intracellular proteins to carry out the cell death program/apoptosis. The activities of effector caspase (caspase 3) and initiator caspase (caspase 9) were analyzed in MG63 and NIH3T3 cells after treatment with complexes **1** and **2** (Fig. 8a). Significant 6-fold increase in caspase 3 and 9 activities were observed in MG63 cells treated with complex **1** and **2** when compared to NIH3T3. Basal minimum caspase 3 and 9 activity was observed in control cells. The results clearly indicate dominance of caspase dependent apoptotic event with eventual cell death [75]. The complexes brought about cell specific apoptosis in osteosarcoma cell line MG-63 when compared to control normal fibroblast cell line, NIH3T3. We further analyzed caspase 8 activity to better understand the specific apoptotic

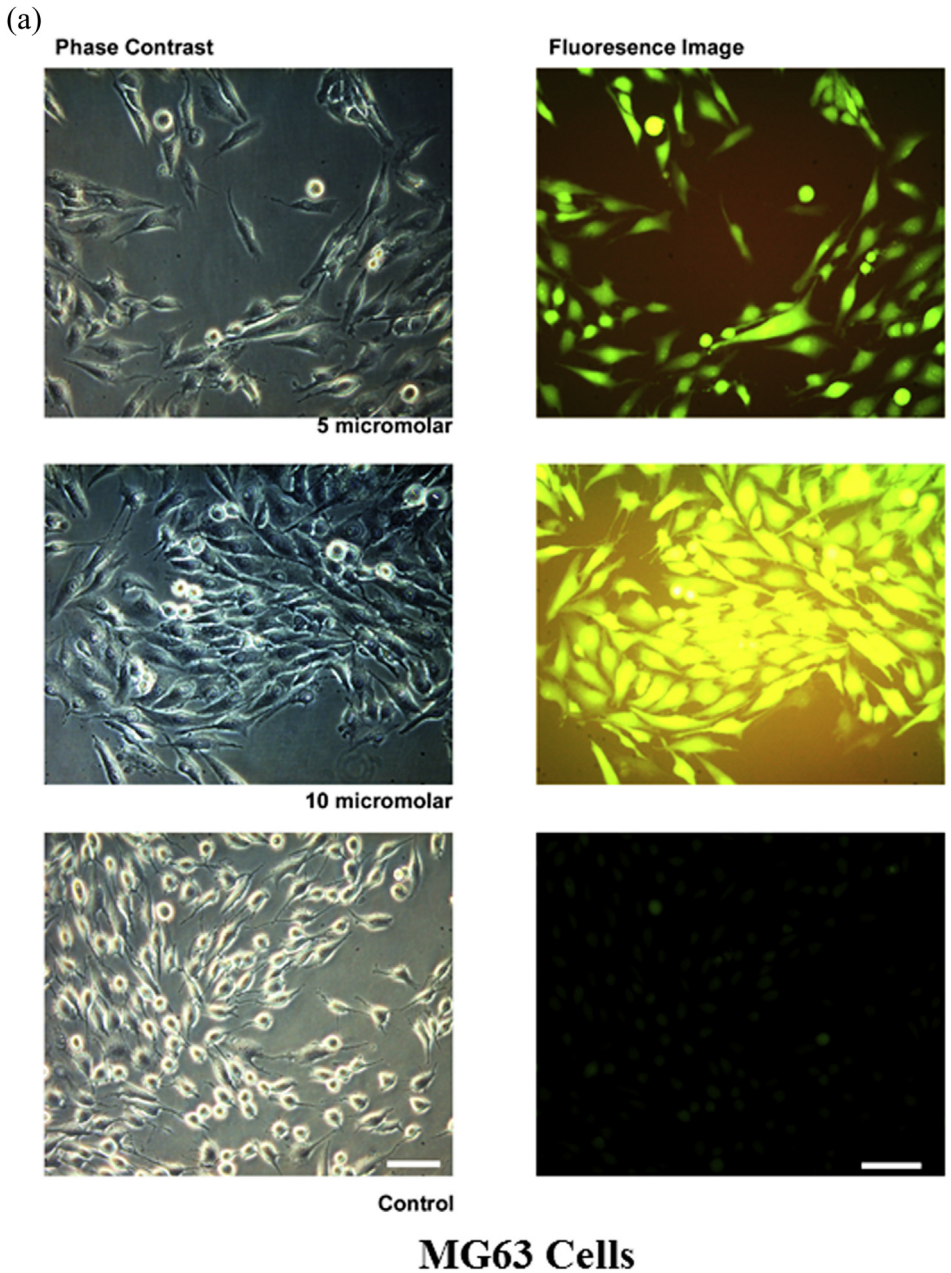

Fig. 9. (a) Morphological changes observed in the MG63 cell line on treatment with complex **1** using DCFH-DA fluorescence microscopic assay. (b) Morphological changes observed in the NIH3T3 cell lines on treatment with complex **1** using DCFH-DA fluorescence microscopic assay.

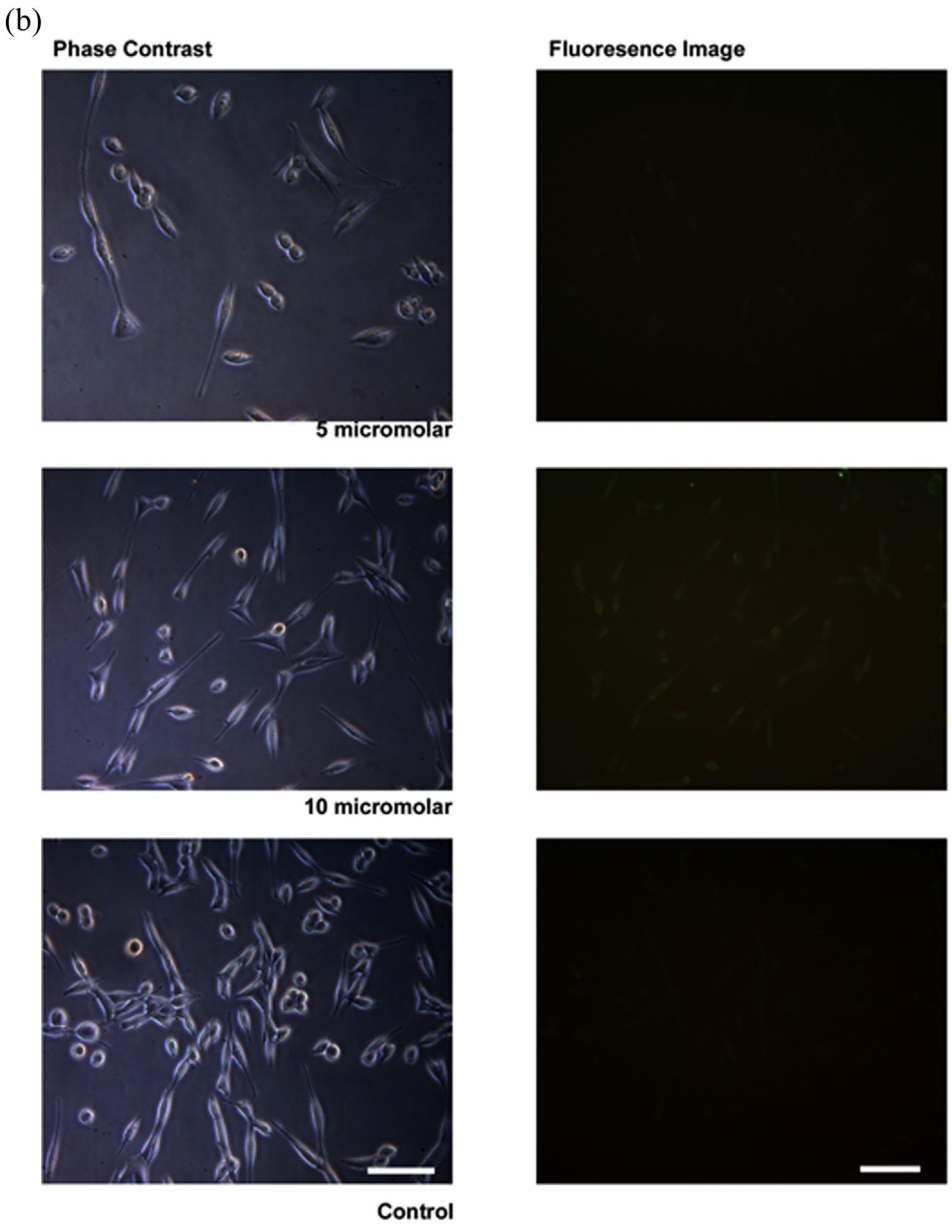

Fig. 9. (*continued*).

pathway utilized by complexes **1** and **2** to mediate their anti-proliferative effect. The two major pathways of apoptosis are referred to as the intrinsic and extrinsic pathways [76]. Depending on the type of apoptotic pathways, specific caspases are activated. In the case of intrinsic pathway, caspase 9 serves as the initiator caspase [77]. Subsequently, caspase 9 activates the downstream effector caspases, namely 3, 6 and 7; whereas in the case of extrinsic pathway, caspase 8 is the initiator caspase which consequently activates effector caspases. The intrinsic pathway gets activated due to oxidant challenge, DNA damage and mitochondrial dysfunction. The extrinsic pathway usually results from activation of death-domain receptors (such as TNF-R, IL-R, Fas, and TNF-related apoptosis inducing ligand-R) leading to formation of a death-inducing signaling complex that activates caspase 8 [78]. The results of caspase 8 activity in NIH3T3 and MG63 cells indicate that treatment with complex **1** and **2** (Fig. 8b) had no effect on the activity of caspase 8 when compared to the untreated controls. The results observed were similar in both NIH3T3 and MG63 cells indicating activation of intrinsic pathway upon treatment with the two copper(II) complexes. In order to further understand whether complexes **1** and **2** mediate the intrinsic pathway of apoptosis by inducing oxidant challenge in the cells, the cells were treated with 2′,7′-dichlorodihydrofluorescein diacetate (DCFH-DA) and the redox state of a cell was analyzed by fluorescence microscopy. DCFH-DA is a cell permeable, relatively non fluorescent molecule, which is sensitive to changes in the redox state of a cell. Activity of cellular esterases cleaves DCFH-DA into 2′,7′-dichlorodihydro-fluorescein ($DCFH_2$), which gets oxidized to 2′,7′-dichloro-fluorescein (DCF) in the presence of free radicals in a cell. Accumulation of DCF in cells may be measured by an increase in

fluorescence at 530 nm when the sample is excited at 485 nm. The oxidant challenge is directly proportional to the green fluorescence intensity from the cells. The microphotograph indicates that treatment with even 5 μM complex **1** induced oxidative stress in MG63 cells (Fig. 9a), when compared to NIH3T3 cells (Fig. 9b). A concentration dependent increase in oxidative stress was seen in cells on treatment with complex **1**. The results indicate that complex **1** induces apoptosis via intrinsic pathway by inducing oxidative stress in the cells and exhibits selectivity in mediating this effect in terms of targeting cancerous cell line when compared to normal fibroblast cell line. On the contrary, significant oxidant challenge to both NIH3T3 and MG63 cells was observed upon treatment with complex **2** even at concentration as low as 5 μM. We did not observe any selectivity of complex **2** in targeting cancerous cells (Supplementary information Fig. S7). However, the effect it mediated in inducing oxidative stress was similar for both NIH3T3 and MG63 cell lines.

3.5.4. Hemolytic assay

Each drug (from lower to higher concentration) needs to be analyzed for its hemolytic potential. Drug-induced hemolysis is a serious toxicity liability [79]. The phenomenon occurs by two mechanisms namely by toxic hemolysis due to direct toxicity of the drug and its metabolite or due to allergic hemolysis due to toxicity caused by an immunological reaction. For any compound to serve as an effective drug, it should resist hemolysis. Hence, complexes **1**–**3** were also tested for their hemolytic activity. All the three complexes with varying concentration were examined for their hemolytic ability (data not shown). It is appropriate to state at this point that complexes **1** and **2** caused no hemolysis.

4. Conclusion

Three copper(II) complexes, complexes **1**, **2** and **3** having a common bitpy ligand but differing with respect to other coligands and coordination number were synthesized and characterized. Complex **1,** a six coordinate complex is a bis chelate with two bitpy ligands coordinated to copper(II) ion. Complex **2** is a five coordinate mixed ligand complex coordinated to a tridentate ligand bitpy and a bidentate ligand phen. On the other hand, complex **3** is a four coordinate complex with a tridentate bitpy ligand and a nitrate ion coordinated to copper(II) ion. All the three complexes exhibited intercalative mode of binding to CT DNA. Similar DNA binding constant, K_b was observed in all the three cases because of the fact that binding of the complexes to DNA was through π-stacking of the planar benzimidazolyl head group on the tridentate ligand bitpy (present in the three complexes) in between the base pairs of DNA. Complexes **1** and **2** exhibited greater DNA condensing ability when compared to complex **3**. Electrophoretic mobility assay showed that DNA condensing ability of complex **2**, which is a mixed ligand complex, was better than that observed for complex **1**. It was of great importance to note that the DNA condensing ability of the three complexes was reversible. Among the three complexes, complex **1** and **2** showed greater antiproliferative effect on MG63 cell line as compared to NIH3T3 cell line. On the other hand, antiproliferative effect of complex **3** on both MG63 and NIH3T3 cell lines was almost similar. Annexin V- Propidium iodide staining experiments and effect of complexes **1** and **2** on caspase 3 and 9 activities further confirmed that cell death brought about by these two complexes in MG-63 cell line was due to apoptosis. Furthermore, caspase 8 assay confirmed that amongst two complexes, complex **1** induced apoptosis by inducing oxidative stress in the cells (intrinsic pathway) and exhibited selectivity in mediating this effect towards MG63 cancerous fibroblast cell line when compared to the normal fibroblast cell line. Collectively, with no effect of the three copper(II) complexes on red blood cells, reversible DNA condensing ability and potent selective cytotoxic effects of complexes **1** and **2**, especially challenging selectivity of complex **1**, it is highly appropriate to state that $[Cu(bitpy)_2](ClO_4)_2$ can be further developed as a potential multimodal therapeutic agent against cancer.

Acknowledgments

One of the authors, S.R wishes to thank CSIR for Senior Research Fellowship. The research support from CSIR XII Plan project STRAIT is acknowledged. CLRI Communication Number: 1058.

Appendix A. Supplementary data

Supplementary data related to this article can be found at http://dx.doi.org/10.1016/j.ejmech.2014.04.064.

References

[1] P. Pil, S.J. Lippard, in: R.B. Joseph (Editor-in-Chief), Cisplatin and Related Drugs, Encyclopedia of Cancer, second ed., Academic Press, New York, 2002, pp. 525–543.
[2] V. Brabec, DNA modifications by antitumor platinum and ruthenium compounds: their recognition and repair, Progress in Nucleic Acid Research and Molecular Biology, Academic Press (2002) 1–68.
[3] V. Brabec, J. Kasparkova, Modifications of DNA by platinum complexes: relation to resistance of tumors to platinum antitumor drugs, Drug Resistance Updates 8 (2005) 131–146.
[4] W. Ginzinger, G. Mahlgassner, V.B. Arion, M.A. Jakupec, A. Roller, M. Galanski, M. Reithofer, W. Berger, B.K. Keppler, A SAR study of novel antiproliferative ruthenium and osmium complexes with quinoxalinone ligands in human cancer cell lines, Journal of Medicinal Chemistry 55 (2012) 3398–3413.
[5] D.-L. Ma, C.-M. Che, F.-M. Siu, M. Yang, K.-Y. Wong, DNA binding and cytotoxicity of ruthenium(II) and rhenium(I) complexes of 2-amino-4-phenylamino-6-(2-pyridyl)-1,3,5-triazine, Inorganic Chemistry 46 (2007) 740–749.
[6] A.M. Pizarro, P.J. Sadler, Unusual DNA binding modes for metal anticancer complexes, Biochimie 91 (2009) 1198–1211.
[7] P.C.A. Bruijnincx, P.J. Sadler, New trends for metal complexes with anticancer activity, Current Opinion in Chemical Biology 12 (2008) 197–206.
[8] N. Farrell, in: J.A. McCleverty, T.J. Meyer (Editors-in-Chief), Metal Complexes as Drugs and Chemotherapeutic Agents, Comprehensive Coordination Chemistry II, Pergamon, Oxford, 2003, pp. 809–840.
[9] M.R. Kaluderovic, G.N. Kaluderovic, S. Gomez-Ruiz, R. Paschke, A. Hemprich, J. Kahling, T.W. Remmerbach, Organogallium(III) complexes as apoptosis promoting anticancer agents for head and neck squamous cell carcinoma (HNSCC) cell lines, Journal of Inorganic Biochemistry 105 (2011) 164–170.
[10] C.X. Zhang, S.J. Lippard, New metal complexes as potential therapeutics, Current Opinion in Chemical Biology 7 (2003) 481–489.
[11] S.S. Bhat, A.A. Kumbhar, H. Heptullah, A.A. Khan, V.V. Gobre, S.P. Gejji, V.G. Puranik, Synthesis, electronic structure, DNA and protein binding, DNA cleavage, and anticancer activity of fluorophore-labeled copper(II) complexes, Inorganic Chemistry 50 (2011) 545–558.
[12] J. Easmon, G. Purstinger, G. Heinisch, T. Roth, H.H. Fiebig, W. Holzer, W. Jager, M. Jenny, J. Hofmann, Synthesis, cytotoxicity, and antitumor activity of copper(II) and iron(II) complexes of 4N-azabicyclo[3.2.2]nonane thiosemicarbazones derived from acyl diazines, Journal of Medicinal Chemistry 44 (2001) 2164–2171.
[13] Y. Ma, L. Cao, T. Kawabata, T. Yoshino, B.B. Yang, S. Okada, Cupric nitrilotriacetate induces oxidative DNA damage and apoptosis in human leukemia HL-60 cells, Free Radical Biology & Medicine 25 (1998) 568–575.
[14] Z. Afrasiabi, E. Sinn, S. Padhye, S. Dutta, S. Padhye, C. Newton, C.E. Anson, A.K. Powell, Transition metal complexes of phenanthrenequinone thiosemicarbazone as potential anticancer agents: synthesis, structure, spectroscopy, electrochemistry and in vitro anticancer activity against human breast cancer cell-line, T47D, Journal of Inorganic Biochemistry 95 (2003) 306–314.
[15] D. Senthil Raja, N.S.P. Bhuvanesh, K. Natarajan, Effect of N(4)-phenyl substitution in 2-oxo-1,2-dihydroquinoline-3-carbaldehyde semicarbazones on the structure, DNA/protein interaction, and antioxidative and cytotoxic activity of Cu(II) complexes, Inorganic Chemistry 50 (2011) 12852–12866.
[16] D. Senthil Raja, N.S.P. Bhuvanesh, K. Natarajan, DNA binding, protein interaction, radical scavenging and cytotoxic activity of 2-oxo-1,2-dihydroquinoline-3-carbaldehyde(2,2'-hydroxybenzoyl)hydrazone and its Cu(II) complexes: a structure activity relationship study, Inorganica Chimica Acta 385 (2012) 81–93.
[17] T.B. Thederahn, M.D. Kuwabara, T.A. Larsen, D.S. Sigman, Nuclease activity of 1,10-phenanthroline-copper: kinetic mechanism, Journal of the American Chemical Society 111 (1989) 4941–4946.

[18] M.E. Katsarou, E.K. Efthimiadou, G. Psomas, A. Karaliota, D. Vourloumis, Novel copper(II) complex of N-propyl-norfloxacin and 1,10-phenanthroline with enhanced antileukemic and DNA nuclease activities, Journal of Medicinal Chemistry 51 (2008) 470–478.

[19] Q.-q. Zhang, F. Zhang, W.-g. Wang, X.-I. Wang, Synthesis, crystal structure and DNA binding studies of a binuclear copper(II) complex with phenanthroline, Journal of Inorganic Biochemistry 100 (2006) 1344–1352.

[20] R.N. Patel, N. Singh, K.K. Shukla, J. Nicols-Gutierrez, A. Castineiras, V.G. Vaidyanathan, B.U. Nair, Characterization and biological activities of two copper(II) complexes with diethylenetriamine and 2,2'-bipyridine or 1,10-phenanthroline as ligands, Spectrochimica Acta A 62 (2005) 261–268.

[21] B. Sun, J.-X. Guan, L. Xu, B.-L. Yu, L. Jiang, J.-F. Kou, L. Wang, X.-D. Ding, H. Chao, L.-N. Ji, DNA condensation induced by ruthenium(II) polypyridyl complexes [Ru(bpy)2(PIPSH)]2+ and [Ru(bpy)2(PIPNH)]2+, Inorganic Chemistry 48 (2009) 4637–4639.

[22] X. Dong, X. Wang, Y. He, Z. Yu, M. Lin, C. Zhang, J. Wang, Y. Song, Y. Zhang, Z. Liu, Y. Li, Z. Guo, Reversible DNA condensation induced by a tetranuclear nickel(II) complex, Chemistry: A European Journal 16 (2010) 14181–14189.

[23] C.-F. Ke, S. Hou, H.-Y. Zhang, Y. Liu, K. Yang, X.-Z. Feng, Controllable DNA condensation through cucurbit[6]uril in 2D pseudopolyrotaxanes, Chemical Communications (2007) 3374–3376.

[24] D.S. Sigman, A. Mazumder, D.M. Perrin, Chemical nucleases, Chemical Reviews 93 (1993) 2295–2316.

[25] X. Qiao, Z.-Y. Ma, C.-Z. Xie, F. Xue, Y.-W. Zhang, J.-Y. Xu, Z.-Y. Qiang, J.-S. Lou, G.-J. Chen, S.-P. Yan, Study on potential antitumor mechanism of a novel Schiff base copper(II) complex: synthesis, crystal structure, DNA binding, cytotoxicity and apoptosis induction activity, Journal of Inorganic Biochemistry 105 (2011) 728–737.

[26] S. Banerjee, S. Mondal, S. Sen, S. Das, D.L. Hughes, C. Rizzoli, C. Desplanches, C. Mandal, S. Mitra, Four new dinuclear Cu(ii) hydrazone complexes using various organic spacers: syntheses, crystal structures, DNA binding and cleavage studies and selective cell inhibitory effect towards leukemic and normal lymphocytes, Dalton Transactions: An International Journal of Inorganic Chemistry (2009) 6849–6860.

[27] A. Kellett, O. Howe, M. O'Connor, M. McCann, B.S. Creaven, S.N. McClean, A. Foltyn-Arfa Kia, A. Casey, M. Devereux, Radical-induced DNA damage by cytotoxic square-planar copper(II) complexes incorporating o-phthalate and 1,10-phenanthroline or 2,2'-dipyridyl, Free Radical Biology and Medicine 53 (2012) 564–576.

[28] M.S. Balakrishna, D. Suresh, A. Rai, J.T. Mague, D. Panda, Dinuclear copper(I) complexes containing cyclodiphosphazane derivatives and pyridyl ligands: synthesis, structural studies, and antiproliferative activity toward human cervical and breast cancer cells, Inorganic Chemistry 49 (2010) 8790–8801.

[29] A. De Vizcaya-Ruiz, A. Rivero-Muller, L. Ruiz-Ramirez, J.A. Howarth, M. Dobrota, Hematotoxicity response in rats by the novel copper-based anticancer agent: casiopeina II, Toxicology 194 (2003) 103–113.

[30] J.M. McCord, I. Fridovich, Superoxide dismutase, The Journal of Biological Chemistry 244 (1969) 6049–6055.

[31] M. O'Connor, A. Kellett, M. McCann, G. Rosair, M. McNamara, O. Howe, B.S. Creaven, S.N. McClean, A. Foltyn-Arfa Kia, D. O'Shea, M. Devereux, Copper(II) complexes of salicylic acid combining superoxide dismutase mimetic properties with DNA binding and cleaving capabilities display promising chemotherapeutic potential with fast acting in vitro cytotoxicity against cisplatin sensitive and resistant cancer cell lines, Journal of Medicinal Chemistry 55, 1957-1968.

[32] M.E. Bravo-Gomez, J.C. Garca-Ramos, I. Gracia-Mora, L. Ruiz-Azuara, Antiproliferative activity and QSAR study of copper(II) mixed chelate [Cu(N-N)(acetylacetonato)]NO_3 and [Cu(N-N)(glycinato)]NO_3 complexes, (Casiopeinas), Journal of Inorganic Biochemistry 103 (2009) 299–309.

[33] R. Buchtik, Z. Travnicek, J. Vanco, R. Herchel, Z. Dvorak, Synthesis, characterization, DNA interaction and cleavage, and in vitro cytotoxicity of copper(II) mixed-ligand complexes with 2-phenyl-3-hydroxy-4(1H)-quinolinone, Dalton Transactions: An International Journal of Inorganic Chemistry 40 (2011) 9404–9412.

[34] M. Chauhan, K. Banerjee, F. Arjmand, DNA binding studies of novel copper(II) complexes containing l-tryptophan as chiral auxiliary: in vitro antitumor activity of Cu-Sn2 complex in human neuroblastoma cells, Inorganic Chemistry 46 (2007) 3072–3082.

[35] R. Indumathy, T. Weyhermuller, B.U. Nair, Biimidazole containing cobalt(III) mixed ligand complexes: crystal structure and photonuclease activity, Dalton Transactions: An International Journal of Inorganic Chemistry 39 (2010) 2087–2097.

[36] G. Sathyaraj, M. Kiruthika, T. Weyhermuller, B.U. Nair, Ruthenium(II) [3 + 2 + 1] mixed ligand complexes: substituent effect on photolability, photooxidation of bases, photocytotoxicity and photonuclease activity, Dalton Transactions: An International Journal of Inorganic Chemistry 41 (2012) 8460–8471.

[37] H.Y. Shrivastava, M. Kanthimathi, B.U. Nair, Copper(II) complex of a tridentate ligand: an artificial metalloprotease for bovine serum albumin, BBA – General Subjects 1573 (2002) 149–155.

[38] D. Lawrence, V.G. Vaidyanathan, B.U. Nair, Synthesis, characterization and DNA binding studies of two mixed ligand complexes of ruthenium(II), Journal of Inorganic Biochemistry 100 (2006) 1244–1251.

[39] V. Uma, V.G. Vaidyanathan, B.U. Nair, Synthesis, structure, and DNA binding studies of copper(II) complexes of terpyridine derivatives, Bulletin of the Chemical Society of Japan 78 (2005) 845–850.

[40] V.G. Vaidyanathan, B.U. Nair, Synthesis, characterization and DNA binding studies of a ruthenium(II) complex, Journal of Inorganic Biochemistry 91 (2002) 405–412.

[41] V.G. Vaidyanathan, B.U. Nair, Photooxidation of DNA by a cobalt(II) tridentate complex, Journal of Inorganic Biochemistry 94 (2003) 121–126.

[42] S. Rajalakshmi, T. Weyhermuller, M. Dinesh, B.U. Nair, Copper(II) complexes of terpyridine derivatives: a footstep towards development of antiproliferative agent for breast cancer, Journal of Inorganic Biochemistry 117 (2012) 48–59.

[43] L. De Laporte, J. Cruz Rea, L.D. Shea, Design of modular non-viral gene therapy vectors, Biomaterials 27 (2006) 947–954.

[44] J. Yin, X. Meng, S. Zhang, D. Zhang, L. Wang, C. Liu, The effect of a nuclear localization sequence on transfection efficacy of genes delivered by cobalt(II) polybenzimidazole complexes, Biomaterials 33 (2012) 7884–7894.

[45] L. Liu, H. Zhang, X. Meng, J. Yin, D. Li, C. Liu, Dinuclear metal(II) complexes of polybenzimidazole ligands as carriers for DNA delivery, Biomaterials 31 (2010) 1380–1391.

[46] S. Rajalakshmi, M.S. Kiran, V.G. Vaidyanathan, E.R. Azhagiya Singam, V. Subramaniam, B.U. Nair, Investigation of nuclease, proteolytic and antiproliferative effects of copper(II) complexes of thiophenylmethanamine derivatives, European Journal of Medicinal Chemistry 70 (2013) 280–293.

[47] A.A. Spasov, I.N. Yozhitsa, L.I. Bugaeva, V.A. Anisimova, Benzimidazole derivatives: spectrum of pharmacological activity and toxicological properties (a review), Pharmaceutical Chemistry Journal 33 (1999) 232–243.

[48] G.W.V. Cave, C.L. Raston, Efficient synthesis of pyridines via a sequential solventless aldol condensation and Michael addition, Journal of the Chemical Society, Perkin Transactions 1 (2001) 3258–3264.

[49] J.B. Chaires, N. Dattagupta, D.M. Crothers, Studies on interaction of anthracycline antibiotics and deoxyribonucleic acid: equilibrium binding studies on the interaction of daunomycin with deoxyribonucleic acid, Biochemistry 21 (1982) 3933–3940.

[50] G. Cohen, H. Eisenberg, Viscosity and sedimentation study of sonicated DNA–proflavine complexes, Biopolymers 8 (1969) 45–55.

[51] J. Marmur, A procedure for the isolation of deoxyribonucleic acid from microorganisms, Journal of Molecular Biology 3 (1961) 208–218.

[52] M.E. Reichmann, S.A. Rice, C.A. Thomas, P. Doty, A further examination of the molecular weight and size of desoxypentose nucleic acid, Journal of the American Chemical Society 76 (1954) 3047–3053.

[53] A.S. Keston, R.B. Brandt, The fluorometric analysis of ultramicro quantities of hydrogen peroxide, Analytical Biochemistry 11 (1965) 1–5.

[54] V. Uma, M. Kanthimathi, T. Weyhermuller, B.U. Nair, Oxidative DNA cleavage mediated by a new copper (II) terpyridine complex: crystal structure and DNA binding studies, Journal of Inorganic Biochemistry 99 (2005) 2299–2307.

[55] S. Rajalakshmi, T. Weyhermuller, A.J. Freddy, H.R. Vasanthi, B.U. Nair, Anomalous behavior of pentacoordinate copper complexes of dimethylphenanthroline and derivatives of terpyridine ligands: studies on DNA binding, cleavage and apoptotic activity, European Journal of Medicinal Chemistry 46 (2011) 608–617.

[56] V. Uma, M. Elango, B.U. Nair, Copper(II) terpyridine complexes: effect of substituent on DNA binding and nuclease activity, European Journal of Inorganic Chemistry (2007) 3484–3490.

[57] L. Li, W. Cao, W. Zheng, C. Fan, T. Chen, Ruthenium complexes containing 2,6-bis(benzimidazolyl)pyridine derivatives induce cancer cell apoptosis by triggering DNA damage-mediated p53 phosphorylation, Dalton Transactions: An International Journal of Inorganic Chemistry 41 (2012) 12766–12772.

[58] S.A. Tysoe, R.J. Morgan, A.D. Baker, T.C. Strekas, Spectroscopic investigation of differential binding modes of.DELTA.- and.LAMBDA.-Ru(bpy)2(ppz)2+ with calf thymus DNA, Journal of Physical Chemistry 97 (1993) 1707–1711.

[59] J.K. Barton, A. Danishefsky, J. Goldberg, Tris(phenanthroline)ruthenium(II): stereoselectivity in binding to DNA, Journal of the American Chemical Society 106 (1984) 2172–2176.

[60] P. Sathyadevi, P. Krishnamoorthy, R.R. Butorac, A.H. Cowley, N.S.P. Bhuvanesh, N. Dharmaraj, Effect of substitution and planarity of the ligand on DNA/BSA interaction, free radical scavenging and cytotoxicity of diamagnetic Ni(II) complexes: a systematic investigation, Dalton Transactions: An International Journal of Inorganic Chemistry 40 (2011) 9690–9702.

[61] Q. Wang, W. Li, A. Liu, B. Zhang, F. Gao, S. Li, X. Liao, Binding and photocleavage of a neutral nickel(II) bis(hydrogen pyridine-2,6-dicarboxylato) complex to DNA, Journal of Molecular Structure 985 (2011) 129–133.

[62] P. Uma Maheswari, M. Palaniandavar, DNA binding and cleavage properties of certain tetrammine ruthenium(II) complexes of modified 1,10-phenanthrolines effect of hydrogen-bonding on DNA-binding affinity, Journal of Inorganic Biochemistry 98 (2004) 219–230.

[63] A.M. Polyanichko, V.V. Andrushchenko, E.V. Chikhirzhina, V.I. Vorobev, H. Wieser, The effect of manganese(II) on DNA structure: electronic and vibrational circular dichroism studies, Nucleic Acids Research 32 (2004) 989–996.

[64] V.I. Ivanov, L.E. Minchenkova, A.K. Schyolkina, A.I. Poletayev, Different conformations of double-stranded nucleic acid in solution as revealed by circular dichroism, Biopolymers 12 (1973) 89–110.

[65] P.T. Selvi, M. Palaniandavar, Spectral, viscometric and electrochemical studies on mixed ligand cobalt(III) complexes of certain diimine ligands bound to calf thymus DNA, Inorganica Chimica Acta 337 (2002) 420–428.

[66] H.Y. Shrivastava, T. Ravikumar, N. Shanmugasundaram, M. Babu, B. Unni Nair, Cytotoxicity studies of chromium(III) complexes on human dermal fibroblasts, Free Radical Biology and Medicine 38 (2005) 58–69.

[67] V. Vijayanathan, T. Thomas, T.J. Thomas, DNA nanoparticles and development of DNA delivery vehicles for gene therapy, Biochemistry 41 (2002) 14085–14094.
[68] I.W. Hamley, V. Castelletto, Biological soft materials, Angewandte Chemie 119 (2007) 4524–4538.
[69] Z.-P. Li, Y.-K. Li, Y.-C. Wang, Study of the interaction of hexa-amine cobalt (III) ion with DNA by a resonance light scattering technique and its analytical application, Luminescence 20 (2005) 282–286.
[70] F.F. Safadi, J. Xu, S.L. Smock, R.A. Kanaan, A.-H. Selim, P.R. Odgren, S.C. Marks, T.A. Owen, S.N. Popoff, Expression of connective tissue growth factor in bone: its role in osteoblast proliferation and differentiation in vitro and bone formation in vivo, Journal of Cellular Physiology 196 (2003) 51–62.
[71] B.E. Trump, I.K. Berezesky, S.H. Chang, P.C. Phelps, The pathways of cell death: oncosis, apoptosis, and necrosis, Toxicologic Pathology 25 (1997) 82–88.
[72] S.J. Martin, C.P. Reutelingsperger, A.J. McGahon, J.A. Rader, R.C. van Schie, D.M. LaFace, D.R. Green, Early redistribution of plasma membrane phosphatidylserine is a general feature of apoptosis regardless of the initiating stimulus: inhibition by overexpression of Bcl-2 and Abl, The Journal of Experimental Medicine 182 (1995) 1545–1556.
[73] J.-B. Denault, G.S. Salvesen, Caspases: keys in the ignition of cell death, Chemical Reviews 102 (2002) 4489–4500.
[74] A.J. Henzing, H. Dodson, J.M. Reid, S.H. Kaufmann, R.L. Baxter, W.C. Earnshaw, Synthesis of novel caspase inhibitors for characterization of the active caspase proteome in vitro and in vivo, Journal of Medicinal Chemistry 49 (2006) 7636–7645.
[75] M. Donovan, T.G. Cotter, Control of mitochondrial integrity by Bcl-2 family members and caspase-independent cell death, BBA – Molecular Cell Research 1644 (2004) 133–147.
[76] A.J.M. Watson, Apoptosis and colorectal cancer, Gut 53 (2004) 1701–1709.
[77] N.N. Danial, S.K. Korsmeyer, Cell death: critical control points, Cell 116 (2004) 205–219.
[78] H.L. Li, H. Zhu, C.J. Xu, J.Y. Yuan, Cleavage of BID by caspase 8 mediates the mitochondrial damage in the fas pathway of apoptosis, Cell 94 (1998) 491–501.
[79] J. Dausset, L. Contu, Drug induced hemolysis, Annual Review of Medicine 18 (1967) 55–70.